

## **Electronic Supplementary Information for**

### ***In-situ* fabrication of all amorphous TiO<sub>2</sub>-coupled-MoS<sub>x</sub> photocatalysts for on-demand photocatalytic hydrogen production by UV light**

Qian Dong,<sup>a,b,c</sup> Yongxing Sun,<sup>d</sup> Fang Wang,<sup>\*a,b,c</sup> Zhengguo Zhang,<sup>a,b,c</sup> and Shixiong  
Min<sup>\*a,b,c,d</sup>

<sup>a</sup> School of Chemistry and Chemical Engineering, North Minzu University, Yinchuan, 750021, P. R. China.

<sup>b</sup> Ningxia Key Laboratory of Solar Chemical Conversion Technology, North Minzu University, Yinchuan 750021, P. R. China.

<sup>c</sup> Key Laboratory of Chemical Engineering and Technology, State Ethnic Affairs Commission, North Minzu University, Yinchuan, 750021, P. R. China.

<sup>d</sup> Analysis and Testing Center of Ningxia Hui Autonomous Region, North Minzu University, Yinchuan, 750021, P. R. China.

\*Corresponding authors: [wangfang987@126.com](mailto:wangfang987@126.com) (F. Wang); [sxmin@nun.edu.cn](mailto:sxmin@nun.edu.cn) (S. Min)

## 1. Experimental section

### 1.1 Chemicals and materials

All chemicals were used as received without further purification. Titanium butoxide ( $\text{Ti}(\text{OC}_4\text{H}_9)_4$ , TBOT, >99%) were purchased from Tianjin Yuanli Chemical Co, Ltd.  $\text{TiO}_2$  nanoparticles (P25, 20% rutile and 80% anatase) were purchased from Degussa. Methanol ( $\text{CH}_3\text{OH}$ ,  $\geq 99.5\%$ ) and anhydrous ethanol ( $\text{C}_2\text{H}_5\text{OH}$ ,  $\geq 99.7\%$ ) were purchased from Tianjin Damao Co, Ltd. Sodium sulfide ( $\text{Na}_2\text{S}\cdot 9\text{H}_2\text{O}$ ,  $\geq 98.0\%$ ) was purchased from Tansoole (China). Sodium sulfite ( $\text{Na}_2\text{SO}_3\cdot 9\text{H}_2\text{O}$ ,  $\geq 97.0\%$ ) was purchased from Tianjin Dingshengxin Chemical Industry Co, Ltd.  $(\text{NH}_4)_2\text{MoS}_4$  was synthesized according to a reported procedure.<sup>1</sup> The high-purity nitrogen ( $\text{N}_2$ , 99.999%) and argon (Ar, 99.999%) were purchased from Jinghua Industrial Gas Co, Ltd. Ultrapure water (18.2 M $\Omega$  cm) was obtained from a water purification system (Hitech ECO-S20).

### 1.2 *In-situ* fabrication of *a*-TM photocatalysts and the photocatalytic $\text{H}_2$ evolution experiments

The *a*-TM photocatalysts were *in-situ* prepared in the reaction solution involving the hydrolysis of TBOT and subsequent photochemical reduction of  $(\text{NH}_4)_2\text{MoS}_4$  under UV light irradiation. In a typical procedure, a transparent solution of 0.25 mmol of TBOT dissolved in 25 mL of  $\text{CH}_3\text{OH}$  was dropwise added into a 75 mL of  $\text{CH}_3\text{OH}/\text{H}_2\text{O}$  (25 mL/50 mL) aqueous solution under vigorous stirring, during which the TBOT was slowly hydrolyzed to form amorphous  $\text{TiO}_2$  (*a*- $\text{TiO}_2$ ). Afterward, a certain amount of  $(\text{NH}_4)_2\text{MoS}_4$  (Mo/Ti=0.5, 1.0, 2.0, 3.0, or 4.0 mol %) was dissolved into the above homogenous *a*- $\text{TiO}_2$  suspension. After stirring for 5 min followed by ultrasonication for another 5 min, the as-obtained *a*- $\text{TiO}_2/\text{MoS}_4^{2-}$  suspension was transferred into a 250 mL reaction cell connected to a closed gas circulation and

evacuation system (CEL-SPH2N, CEAULIGHT). After being thoroughly degassed to remove the oxygen inside the reactor, the reaction suspension was illuminated by a 300 W Xe lamp (CELHXF300), during which the  $\text{MoS}_4^{2-}$  was photochemically reduced into  $a\text{-MoS}_x$ , leading to the formation of all-amorphous  $\text{TiO}_2$ -coupled- $\text{MoS}_x$  ( $a\text{-TM}_x$ ) photocatalysts along with the in-situ production of  $\text{H}_2$ , where the  $x$  represents the Mo/Ti molar ratio. During the synthesis and photocatalytic  $\text{H}_2$  evolution processes, the temperature of the reaction system was maintained at 6 °C by cycling a cooled anhydrous ethanol. The amount of  $\text{H}_2$  gas produced was measured by an on-line gas chromatograph (GC). After the photocatalytic  $\text{H}_2$  evolution reaction, the as-fabricated  $a\text{-TM}$  was collected by centrifugation, washed with  $\text{H}_2\text{O}$  and  $\text{C}_2\text{H}_5\text{OH}$ , and finally freeze-dried for following characterizations. For a comparison, the PM photocatalysts were synthesized by using the exact same procedures for the preparation of  $a\text{-TM}$  except using well-crystallized P25 nanoparticles to replace  $a\text{-TiO}_2$ .

To demonstrate the feasibility of the in-situ fabrication of  $a\text{-TM}$  photocatalyst, the preparation of  $a\text{-TM}_2$  was scaled up by simply doubling the amounts of TBOT and  $(\text{NH}_4)_2\text{MoS}_4$  used and tested for the photocatalytic  $\text{H}_2$  evolution in 50 vol%  $\text{CH}_3\text{OH}$ - $\text{H}_2\text{O}$  while keeping all other conditions unchanged. To further demonstrate the feasibility of on-demand  $\text{H}_2$  production, the photocatalytic  $\text{H}_2$  evolution experiment with *in-situ* fabricated  $a\text{-TM}_2$  was also carried out outside the room of chemistry department building of North Minzu University (Yinchuan, Ningxia Hui Autonomous Region) between 10.30 a.m. and 15.30 p.m. on 19 August 2024. The light intensity was measured every 20 min during the experiment and the average light intensity during the experiment was determined to be 54.54 mW.

The photocatalytic  $\text{H}_2$  evolution stability of the samples was evaluated by performing a continuous cycling reaction over a period of 30 h in a 100 mL of 50 vol.%

CH<sub>3</sub>OH solution. After the first cycle reaction, 80 vol.% CH<sub>3</sub>OH was added into the system to maintain the volume of reaction solution to be 100 mL, and the reaction system was thoroughly degassed again and directly tested for the next cycle reaction without separating the photocatalyst.

The apparent quantum yield (AQY) for the photocatalytic H<sub>2</sub> evolution were measured under the conditions similar to the above photocatalytic reaction except the light source was equipped with bandpass filter of 365 nm. The photon flux of incident light was determined using a Ray virtual radiation actinometer (Apogee MQ-500). The AQY is calculated from the ratio of the number of reacted electrons ( $n_e$ ) during H<sub>2</sub> evolution to the number of incident photons ( $n_p$ ) according to Equation (1):

$$\text{AQY (\%)} = \frac{2 \times n_e}{n_p} \times 100 \quad (1)$$

### 1.3 Characterizations

X-ray diffraction (XRD) patterns were analyzed in the  $2\theta$  range of 5~80° with a scanning rate of 10° min<sup>-1</sup> using a Rigaku Smartlab diffractometer with Cu  $K\alpha$  radiation, operating at 40 kV and 40 mA. Scanning electron microscopy (SEM) images were taken with a ZEISS EVO 10 scanning electron microscope. Transmission electron microscopy (TEM) images were taken with a FEI Talos F200x field emission transmission electron microscope. X-ray photoelectron spectroscopy (XPS) measurements of the samples were performed on a Thermo Fisher Escalab-250Xi electron spectrometer using an Al  $K\alpha$  X-ray source. All spectra were calibrated according to the C 1s binding energy at 284.8 eV. The elemental content was determined by inductively coupled plasma-optical emission spectroscopy (ICP-OES) (Optima 7000 DV). UV–vis diffuse reflectance spectra (UV-vis-DRS) were recorded on a PerkinElmer Lambda-750 UV-vis-near-IR spectrometer equipped with an

integrating sphere, and Ba<sub>2</sub>SO<sub>4</sub> powders were used as a reflectance standard. Fourier transform-infrared (FT-IR) spectra were collected from a Thermo Nicolet Avatar 380 instrument. Raman spectra were collected by using a Horiba Evolution Raman spectrometer with a 488 nm laser as an excitation source. The photoluminescence (PL) spectra of the catalysts dispersed in a 50 vol.% CH<sub>3</sub>OH solution upon excitation at 280 nm were measured using a Horiba Science Fluormax-4 fluorescence spectrophotometer.

#### **1.4 Electrochemical and photoelectrochemical measurements**

Electrochemical and photoelectrochemical measurements were carried out in a three-electrode cell using an electrochemical workstation (CHI 760E, Shanghai, China). A Pt mesh (1 cm×1 cm) and a saturated Ag/AgCl electrode were used as the counter and reference electrodes, respectively. A 0.5 M Na<sub>2</sub>SO<sub>4</sub> was used as the supporting electrolyte. The working electrode was fabricated by the drop-coating method as follows: 5 mg photocatalyst powder was first dispersed by ultrasonication into a mixed solution of C<sub>2</sub>H<sub>5</sub>OH (0.5 mL) and H<sub>2</sub>O (1 mL). After that, 0.25 mL of photocatalyst suspension was drop-casted onto the conductive side of a FTO glass (1 cm×1.5 cm), and the obtained electrode was dried in a flow of air and dried at 50 °C for 24 h. The linear sweep voltammetry (LSV) measurements were carried out at a scan rate of 5 mV s<sup>-1</sup>. Electrochemical impedance spectroscopy (EIS) measurements were performed at a bias of 0.5 V vs. Ag/AgCl electrode in the frequency range of 0.01 to 100 kHz with an AC amplitude of 5 mV. For the photoelectrochemical measurements, photocurrents were collected on an inert working electrode (Pt mesh, 1 cm×1 cm) immersed in a 0.5 M Na<sub>2</sub>SO<sub>4</sub> suspension of photocatalyst (0.2 g L<sup>-1</sup>). The photocurrent response was recorded at a 0.5 V bias under continuous light irradiation from a 300-W Xe lamp.

## 2. Additional figures and tables

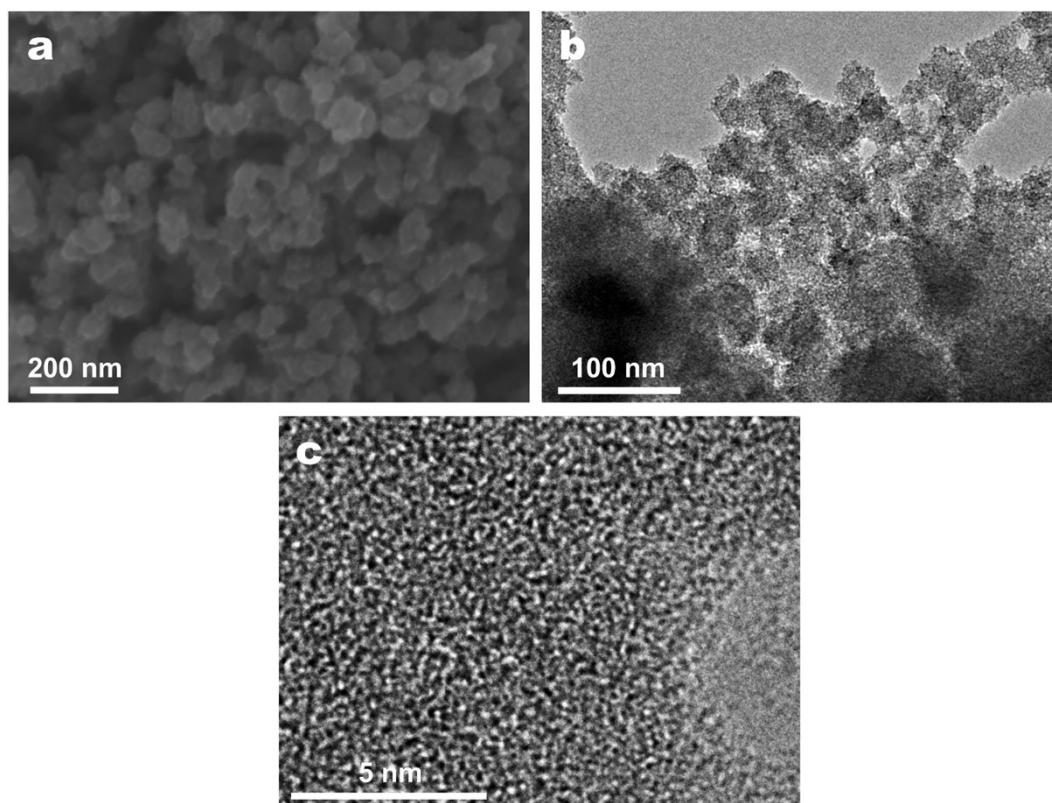


Fig. S1 (a) SEM, (b)TEM, and (c) HRTEM images of *a*-TiO<sub>2</sub>.

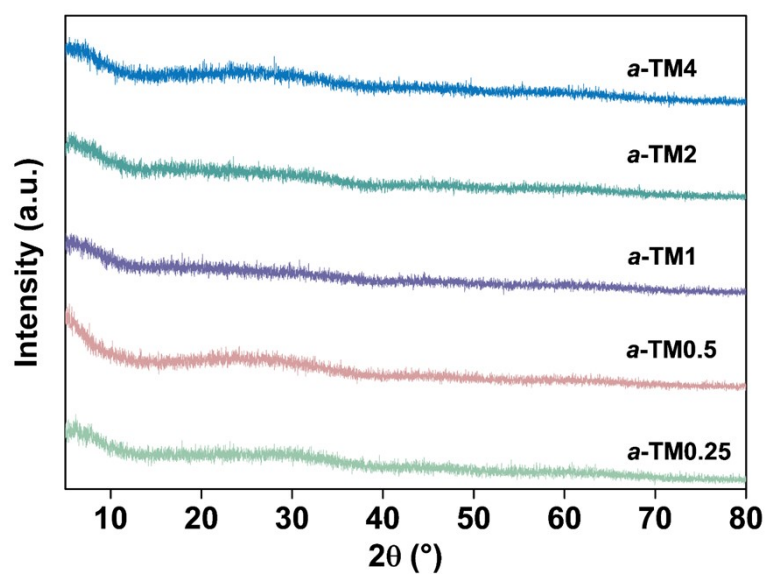


Fig. S2 XRD patterns of *a*-TM photocatalysts.

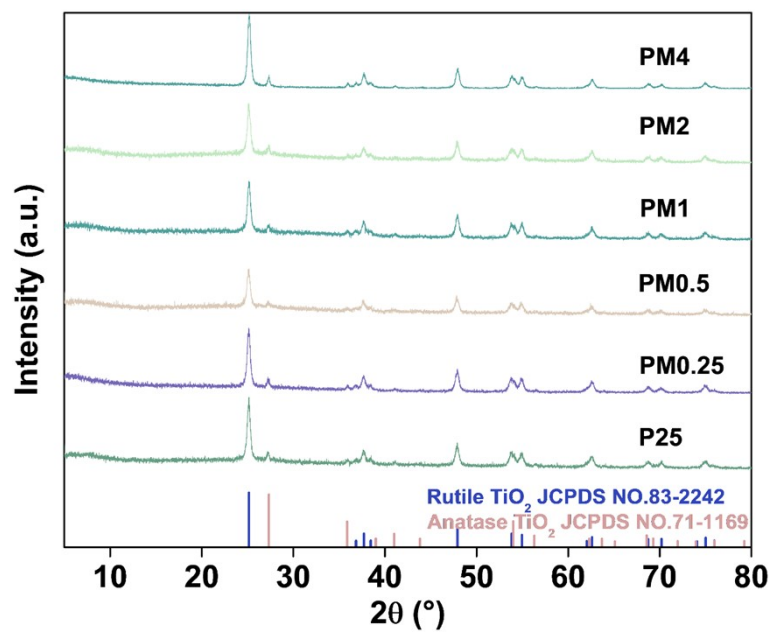


Fig. S3 XRD patterns of PM photocatalysts.

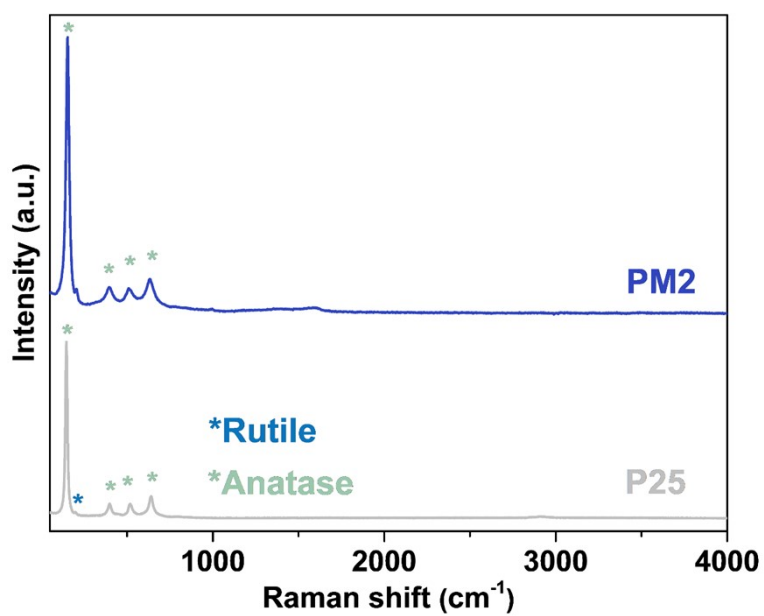
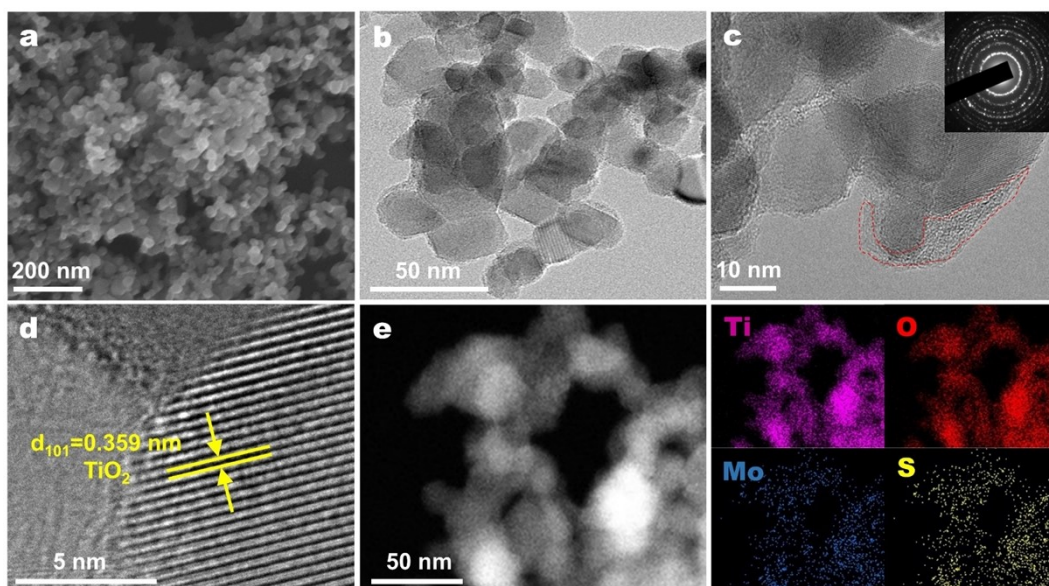
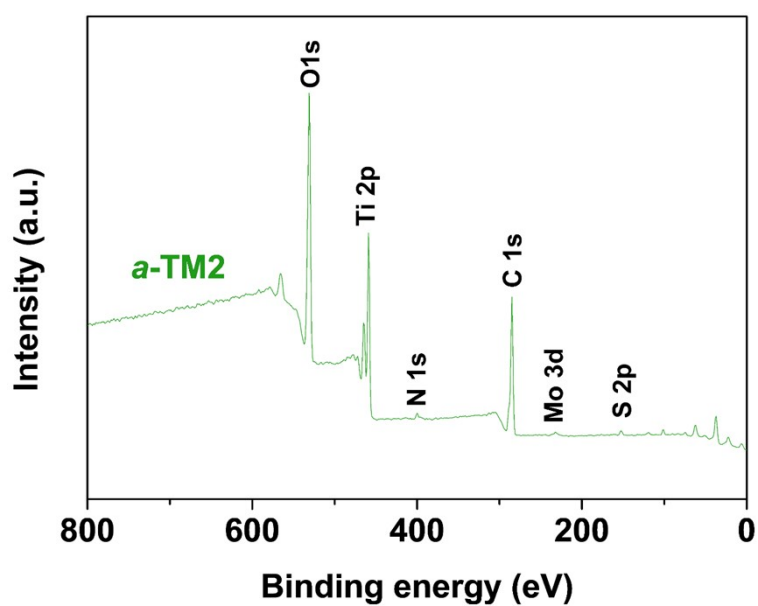


Fig. S4 Raman spectra of P25 and PM2.



**Fig. S5** (a) SEM, (b) TEM, and (c and d) HRTEM images of PM2. The insets in panel (c) showing the corresponding SAED pattern. (e) HAADF-STEM image of PM2 and the corresponding EDX elemental mapping images.



**Fig. S6** XPS survey spectrum of *a*-TM2.



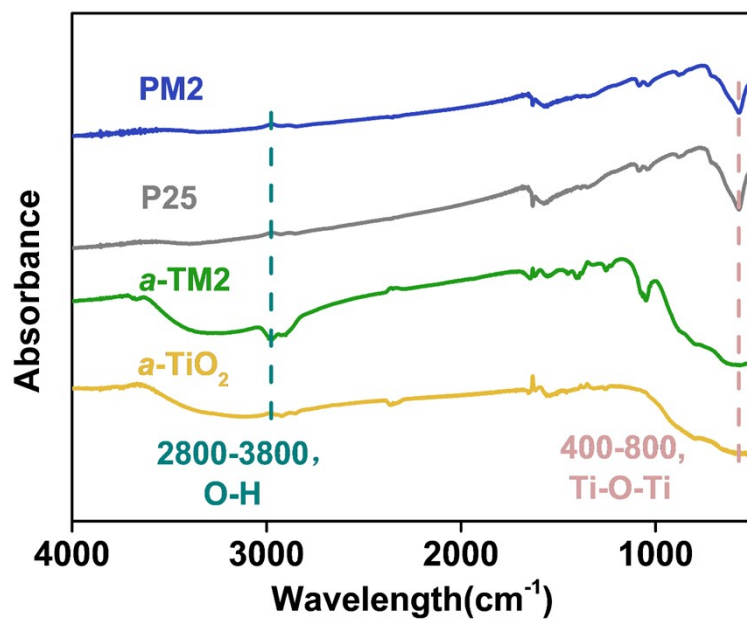


Fig. S7 FT-IR spectra of *a*-TiO<sub>2</sub>, *a*-TM2, P25, and PM2.

**Table S1** Mo content in the *a*-TM photocatalysts determined by the ICP-OES analysis.

Sample	<i>a</i> -TM0.25	<i>a</i> -TM0.5	<i>a</i> -TM1	<i>a</i> -TM2	<i>a</i> -TM4
Mo (wt.%)	0.12	0.27	0.41	0.77	1.48

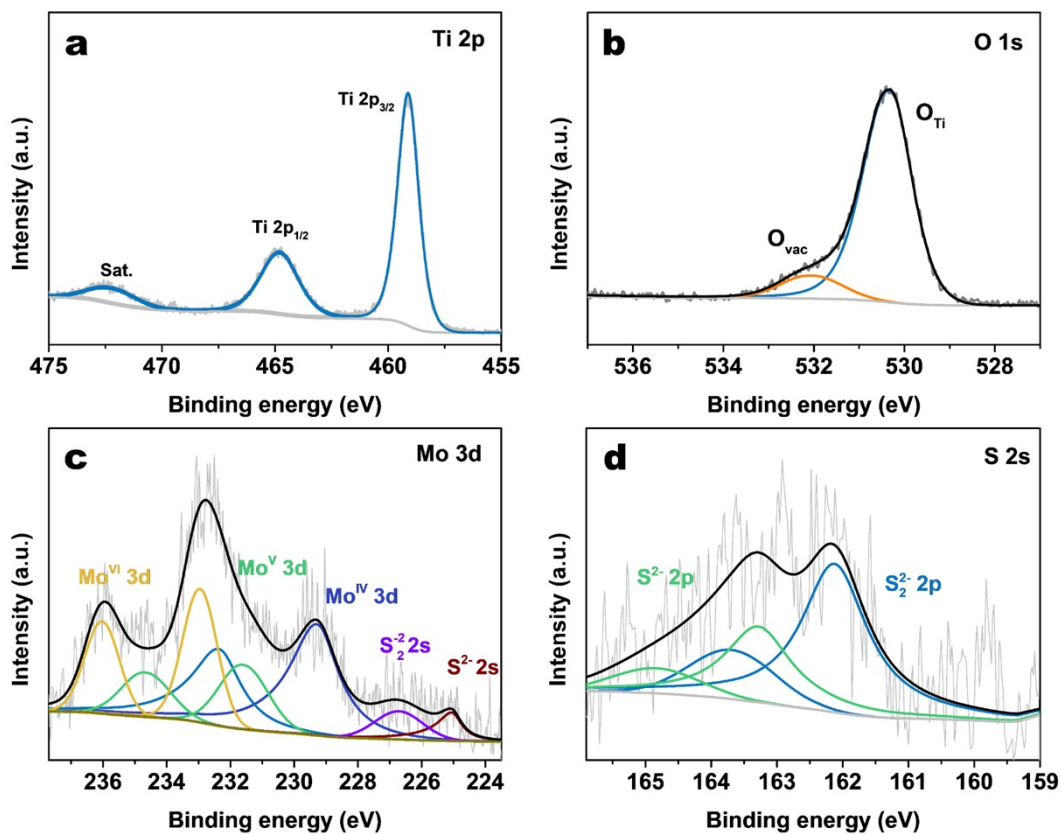


Fig. S8 (a) Ti 2p, (b) O 1s, (c) Mo 3d, and (d) S 2p XPS spectra of PM2.

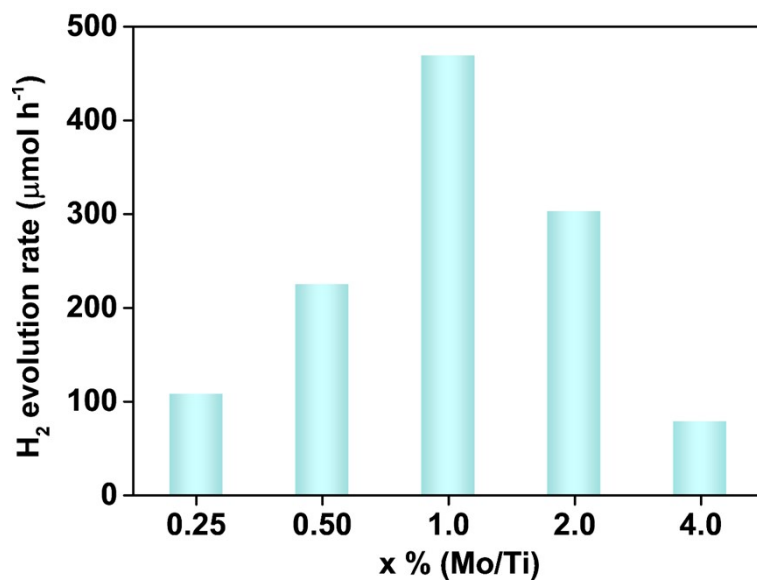


Fig. S9 Effect of Mo:Ti ratio on the photocatalytic HER activity of PM photocatalysts.

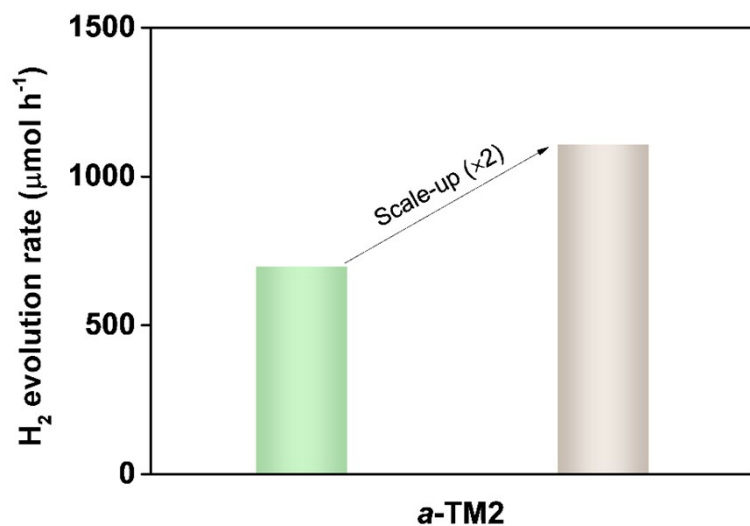


Fig. S10 H<sub>2</sub> evolution activity of *in-situ* fabricated *a*-TM2.

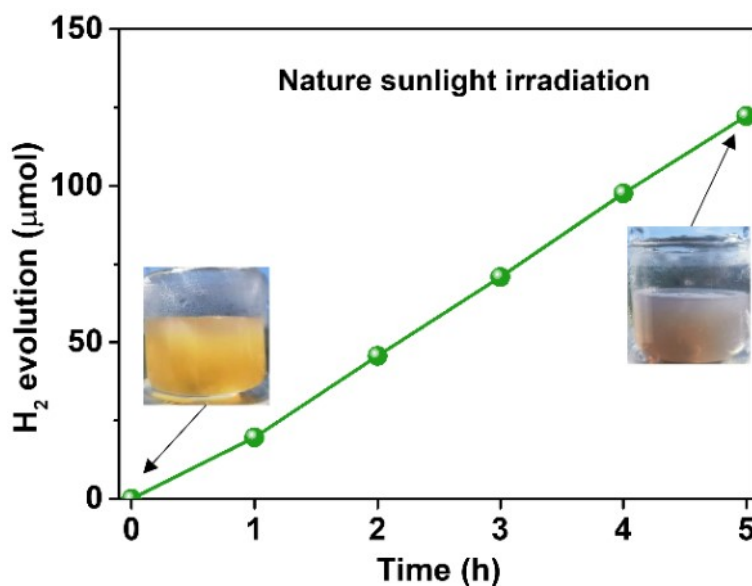
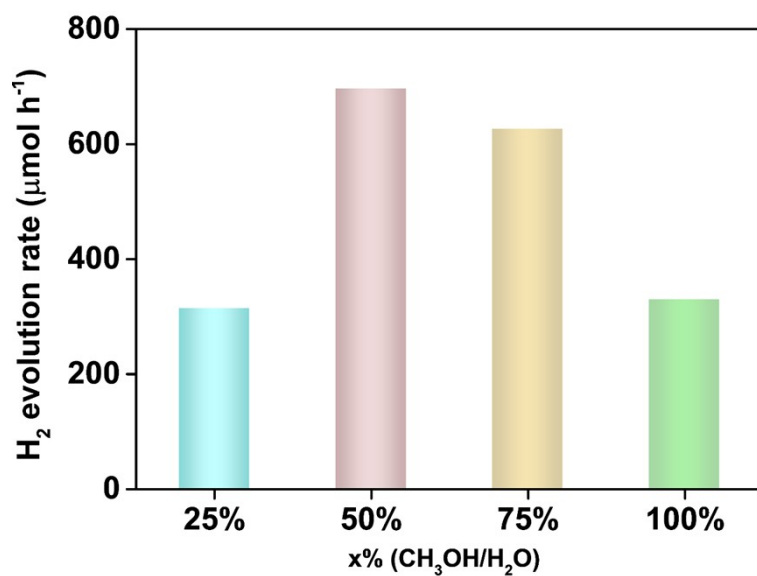
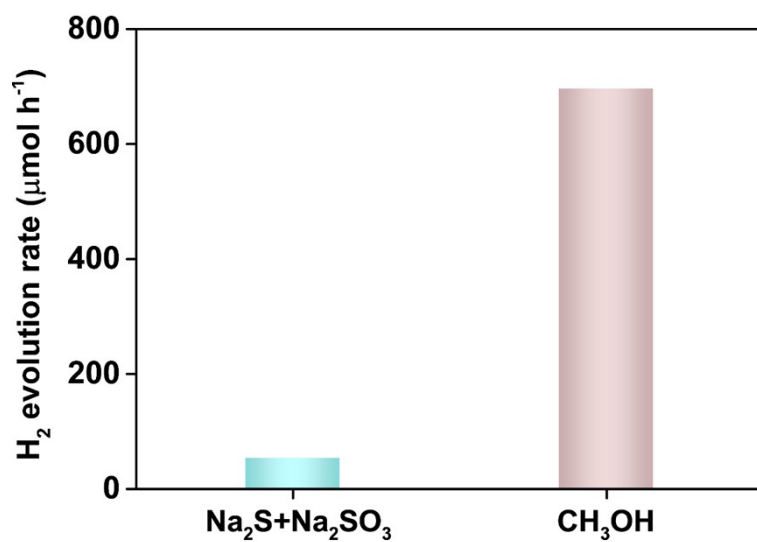


Fig. S11 H<sub>2</sub> evolution activity of *in-situ* fabricated *a*-TM2 under natural sunlight irradiation.



**Fig. S12** Effect of CH<sub>3</sub>OH concentration on the photocatalytic HER activity of *a*-TM2.



**Fig. S13** Photocatalytic HER activities of *a*-TM2 with different sacrificial reagents.

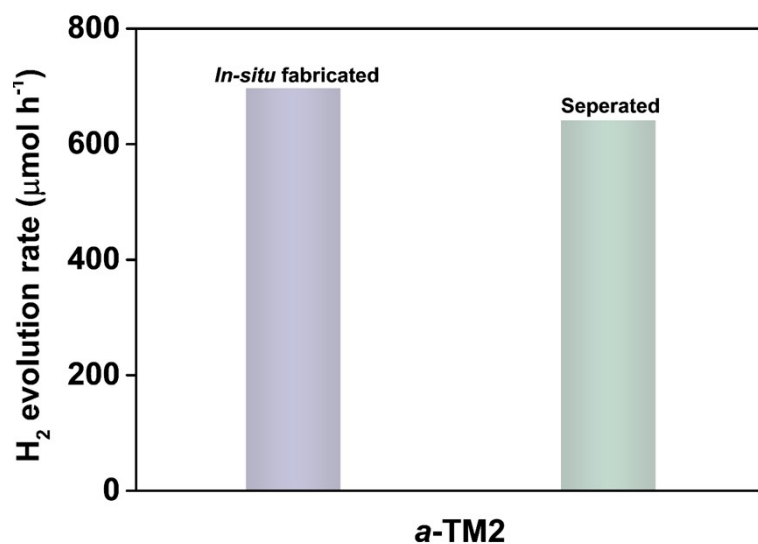


Fig. S14 Photocatalytic HER activities of unseparated and separated *in-situ* fabricated *a*-TM2.

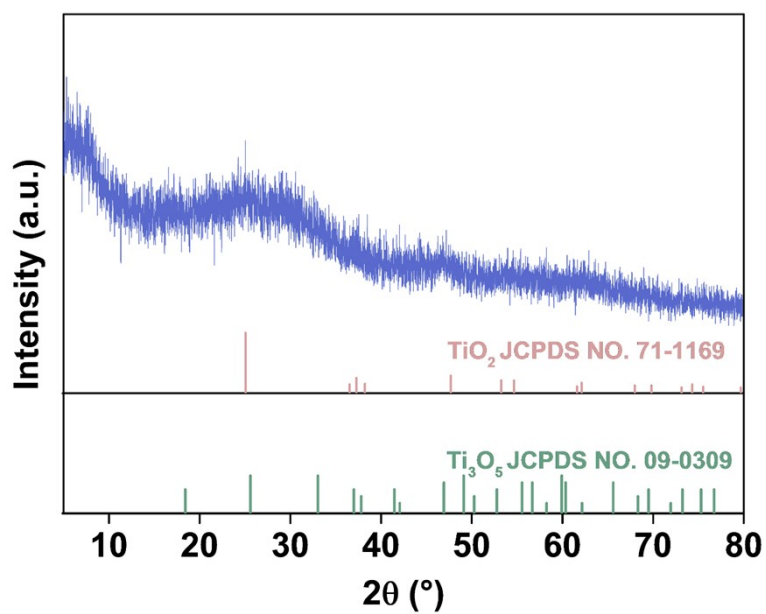
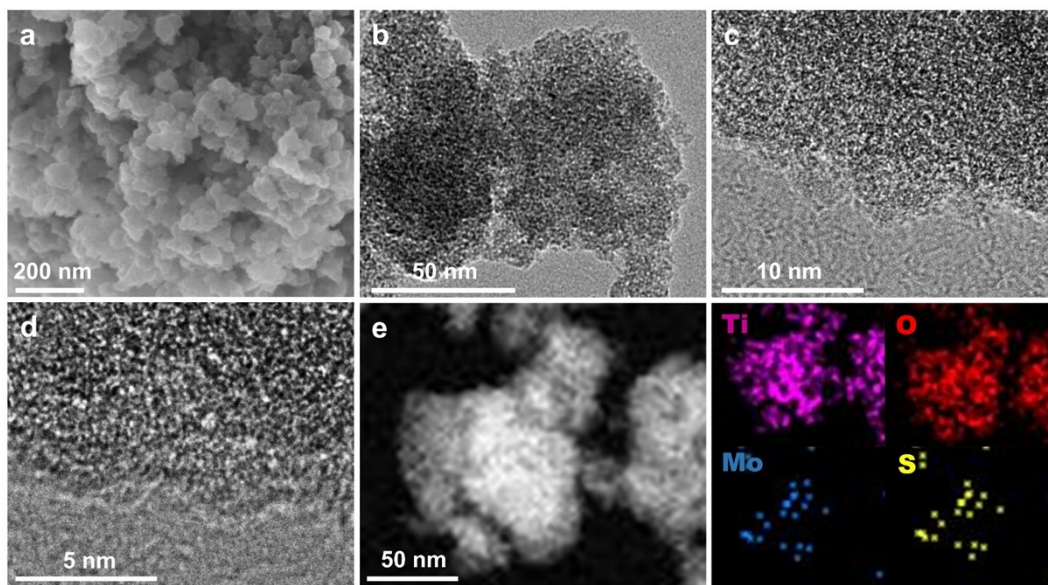
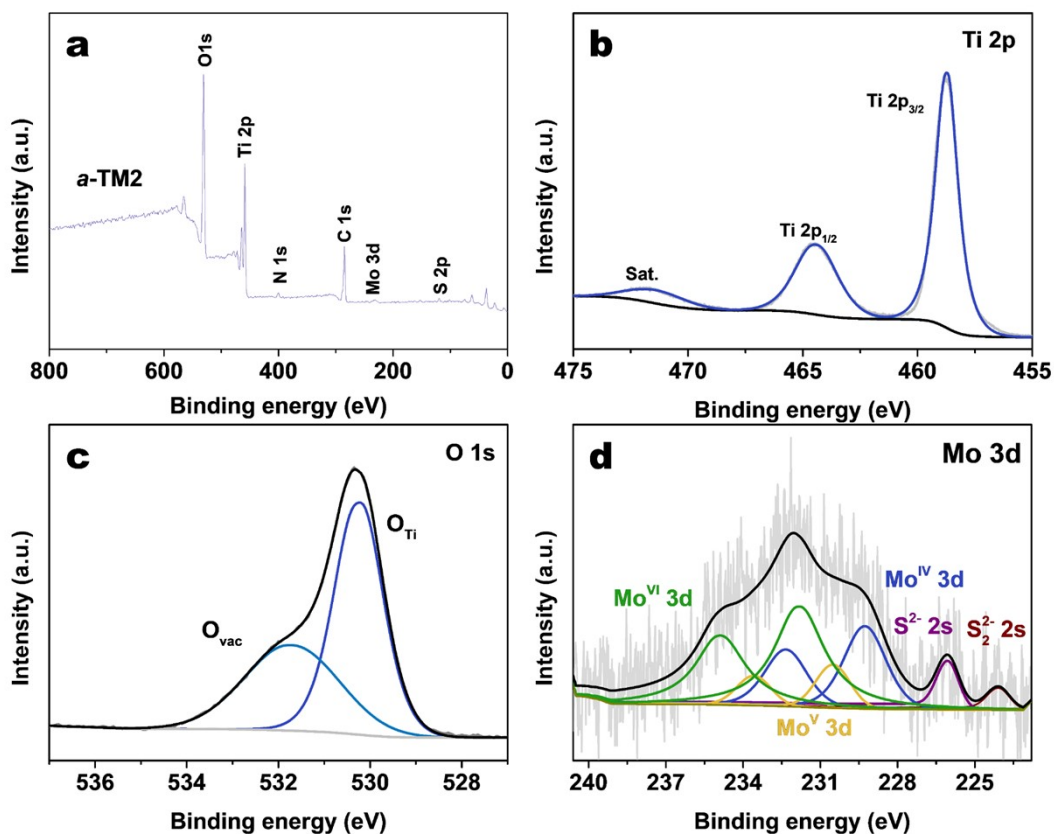


Fig. S15 XRD pattern of *a*-TM2 after the stability test.



**Fig. S16** (a) SEM, (b) TEM, and (c and d) HRTEM images of *a*-TM2 after the stability test. (e) HAADF-STEM image of *a*-TM2 after the stability test and the corresponding EDX elemental mapping images.



**Fig. S17** (a) Survey, (b) Ti 2p, (c) O 1s, and (d) Mo 3d XPS spectra of *a*-TM2 after the stability test.

**Table S2**  $R_{ct}$  values for the photocatalysts obtained by fitting the EIS plots.

Photocatalyst	$R_{ct}$ ( $\Omega$ )	
	Dark	Light
P25	1539.0	555.9
PM2	722.2	198.9
$\alpha$ -TiO <sub>2</sub>	2051.2	566.8
$\alpha$ -TM2	208.3	153.7

### Supplementary References

[S1] X. Zong, Z. Xing, H. Yu, Y. Bai, G. Lu and L. Wang, *J. Catal.*, 2014, **310**, 51.